nature photonics

Article

https://doi.org/10.1038/s41566-026-01962-8

Extensible universal photonic quantum computing with nonlinearity

Received: 28 October 2025

Accepted: 9 June 2026

Published online: 31 July 2026

Check for updates

Shang Yu[1,2,10] ✉, Jinzhao Sun[3,10] ✉, Kuan-Cheng Chen[2,4,10], Zhi-Huai Yang[5,6], Zhenghao Li[1,2], Ewan Mer[1,2], Yazeed K. Alwehaibi[1,2], Shana H. Winston[1,2], Dayne Marcus Lopena[1,2], Zi-Cheng Zhang[7], Guang Yang[6], Runxia Tao[5,6], Mingti Zhou[5,6], Gerard J. Machado[1,2], Ying Dong[5,6] ✉, Roberto Bondesan[2,8], Vlatko Vedral[9], M. S. Kim[1,2], Ian A. Walmsley[1,2] & Raj B. Patel[1,2] ✉

Universal quantum computing requires an architecture that supports both linear circuits and, crucially, strong nonlinear resources. For quantum photonic systems, integrating such nonlinearities with scalable linear circuitry has been a main bottleneck, leaving most optical experiments without nonlinear operations and, consequently, incapable of achieving universality. Here we report on an extensible photonic computer that supports a universal physical gate set by seamlessly combining fully programmable, scalable linear-optical networks with integrated nonlinear modules. This platform enables a broad range of quantum computing and simulation tasks. We demonstrate the quasi-deterministic generation of optical Gottesman–Kitaev–Preskill states, which are essential resources for bosonic error correction yet had previously been realized only probabilistically. Furthermore, we simulate complex many-body quantum dynamics, exemplified by the Bose–Hubbard model. Such quantum simulation tasks have long been considered beyond the reach of photonic hardware limited to linear operations. These capabilities, enabled by our extensible architecture, establish a viable route towards photonic quantum simulation and fault-tolerant quantum computing.

Quantum computing has recently achieved milestone demonstrations across various hardware platforms[1–4], and it is moving towards large-scale quantum computation beyond the noisy intermediate-scale quantum era. Photonic systems[5,6] continue to attract great attention due to advances in architecture[1,7], hardware[3,8], resources for error correction[2,4] and applications[9–11]. The long-term goal of realizing a large-scale fault-tolerant photonic quantum computer requires transversal logic and magic state distillation for the implementation of tailored error-correcting codes, such as the surface code[12]. An immediate experimental challenge lies in developing architectures consisting of a complete physical gate set of linear and nonlinear operations.

Recent experiments have separately demonstrated scalability[1,3,13], programmability in linear optics[3,11] and access to nonlinear operations[14,15]. Historically, optical circuitry in these architectures has been non-universal at the hardware level[16–18], as single-photon-level nonlinearities are intrinsically difficult to realize and even more

[1]Blackett Laboratory, Department of Physics, Imperial College London, London, UK. [2]Centre for Quantum Engineering, Science and Technology (QuEST), Imperial College London, London, UK. [3]School of Physical and Chemical Sciences, Queen Mary University of London, London, UK. [4]Department of Electrical and Electronic Engineering, Imperial College London, London, UK. [5]College of Metrology Measurement and Instrument, China Jiliang University, Hangzhou, China. [6]HeliQ Standard CompuTech Co. Ltd, Hangzhou, China. [7]Department of Physics, The University of Hong Kong, Hong Kong SAR, China. [8]Department of Computing, Imperial College London, London, UK. [9]Clarendon Laboratory, University of Oxford, Oxford, UK. [10]These authors contributed equally: Shang Yu, Jinzhao Sun, Kuan-Cheng Chen. ✉e-mail: shang.yu@imperial.ac.uk; jinzhao.sun.phys@gmail.com; yingdong@cjlu.edu.cn; raj.patel1@imperial.ac.uk

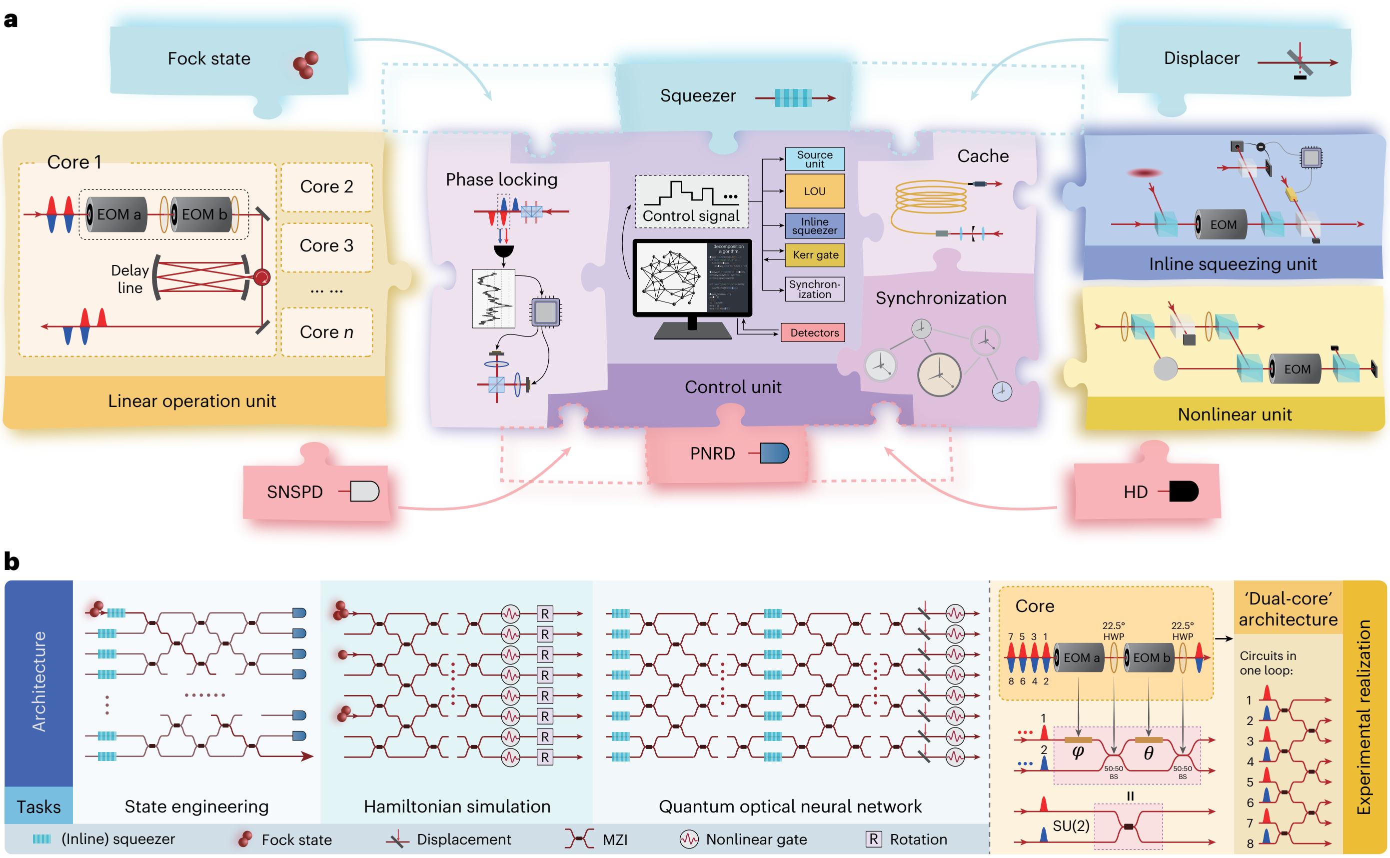

Fig. 1 | An extensible universal photonic quantum computing architecture and example applications. a, Schematic of the architecture. Clavina features jigsaw-like extensibility. A central CU provides phase control, synchronization and long-fibre delay lines that serve as a cache. The LOU, ISU[20] and NLU[15] can be plugged into this CU to expand the scale and functionality of the system. Different light sources (blue pieces) and detectors (red pieces) can be connected individually or simultaneously. This design achieves extensibility by combining mode-count scalability with modular composability. More details are provided in Methods and Supplementary Section I. **b**, Several example applications supported by Clavina. Tasks such as sampling[11,13] and cluster-state generation[28,29] can be directly implemented with its LOU. By integrating non-Gaussian resources, more advanced applications—such as quantum optical neural networks (QONNs)[57], error-correction codes[4,54] and Hamiltonian simulation[58]—also become achievable. See Supplementary Section V for details. The diagram on the right provides a detailed illustration of how the LOU cores enable interactions among qumodes. EOM, electro-optic modulator; BS, beam splitter; HWP, half-wave plate; MZI, Mach–Zehnder interferometer; φ, phase-shift angle; θ, mode-mixing angle; SU(2), special unitary group of degree two.

challenging to implement across all modes in large-scale linear photonic circuits[15,19]. A flexible architecture capable of integrating diverse, function-specific photonic modules is essential for overcoming these challenges.

Inspired by the architecture of classical central processing units (CPUs), a natural approach is to develop an extensible and modular design for quantum processors. In a CPU, a control unit (CU) orchestrates a primary data path—such as an arithmetic logic unit—and routes data via buses to specialized coprocessors (for example, floating-point or graphics units) when complex, dedicated operations are required. Analogously, a CU in a photonic quantum processor could selectively route optical modes between a linear-optical network and specialized nonlinear functional modules. However, achieving this level of modular integration in the quantum regime remains elusive; consequently, current fully programmable circuits are constrained to performing only linear operations[3,8,11,13]. An emerging approach for overcoming this is to exploit time-bin multiplexing within a specially designed cyclic architecture. Akin to the use of CPU registers and iterative instruction pipelining, this method encodes information sequentially along a single path mode. This architecture allows the linear network and costly nonlinear physical modules to be dynamically reused across the circuit, and it applies operations precisely when needed, thus substantially reducing the hardware overhead in large-scale photonic processors.

In this work, we present such an extensible all-optical architecture, Clavina, which integrates a large-scale linear-optical network with plug-and-play nonlinear modules via a central CU. The fully connected, programmable linear network achieves large-scale processing via a multi-core time-bin interferometer. We extended its functionality by interfacing two addressable modules—an inline squeezer[20] and a Kerr interaction module[15]—each of which can be independently enabled or disabled as required. Our design preserves the scalability and programmability of linear operations while incorporating nonlinear resources, so that the system can support a universal gate set[16]. By realizing a universal gate set at the physical level, this architecture enables the future implementation of tailored codes, such as the surface Gottesman–Kitaev–Preskill (GKP) code[12], exploiting transversal gates and magic state distillation for fault-tolerant universal photonic computing.

With this architecture, applications that were previously out of reach or that would require dedicated hardware to run are now unlocked within a single apparatus. As examples, we demonstrate applications relying on processing with linear resources—Gaussian boson sampling and large-scale continuous-variable cluster-state generation—followed by two applications requiring nonlinear operations that leverage the extensibility of Clavina.

Unlike existing probabilistic schemes, Clavina enables the integration of a quantum light source that near-deterministically supplies photon-number-squeezed states. This provides the requisite

https://doi.org/10.1038/s41566-026-01962-8

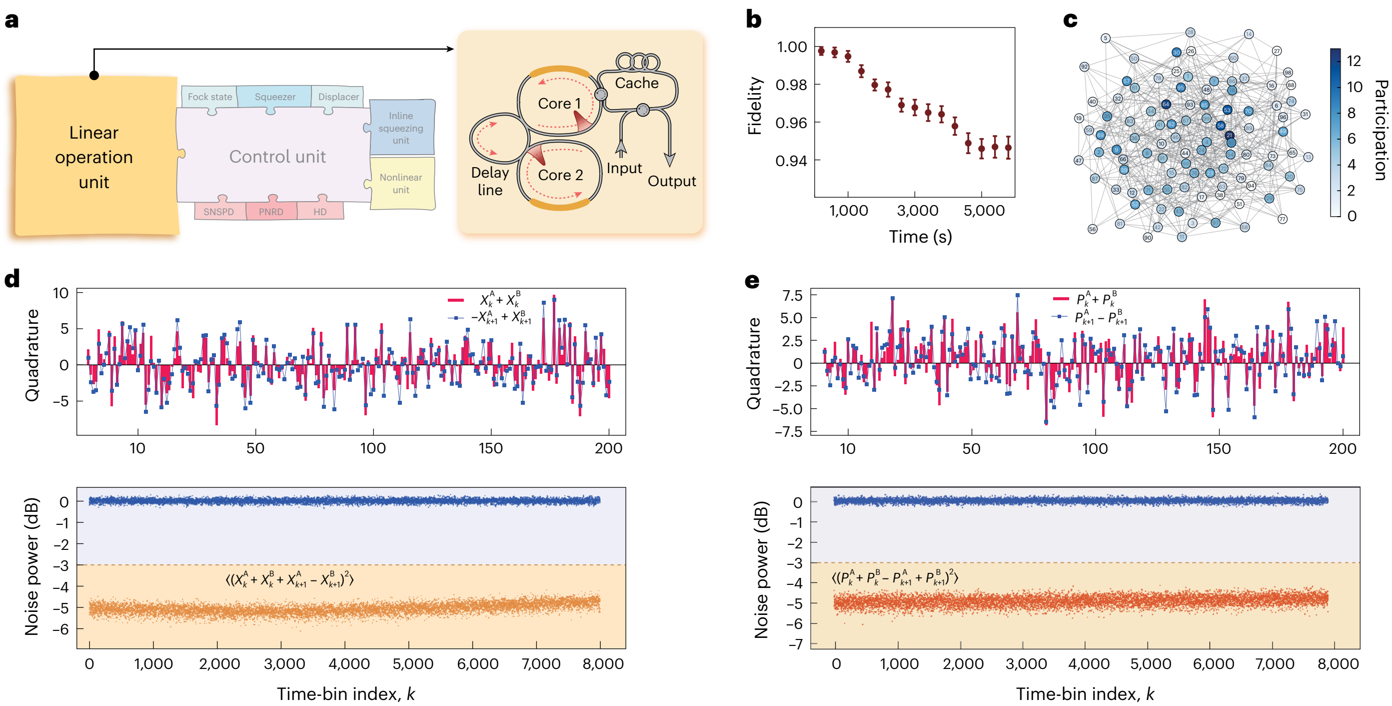

Fig. 2 | Scalability and nonlinearity through modular functional units. **a**, Large-scale linear transformations using the LOU. **b**, By comparing sampling patterns acquired at different times with the initial pattern, we tracked the fidelity over nearly 2 h, which clearly demonstrates the stability of the platform. The points show the mean fidelity at each time, and error bars denote ±1 standard error of the mean over ten independent experimental runs. **c**, The participation coefficients for eight-cliques associated with all nodes in a 100-node network were extracted from Gaussian boson sampling data with more than three photons. **d**,**e**, The quadrature correlations of the cluster state indicate strong x-quadrature correlations (**d**) and p-quadrature correlations (**e**) between modes A and B, corresponding to the odd and even input states shown in the rightmost part of Fig. 1b, across the first 200 time-bin modes. The lower measurements (orange) show that the nullifier variances remained consistently below the −3 dB inseparability threshold over 8,000 modes. The reference shot-noise variances shown in blue confirm the sustained multimode entanglement in both quadratures.

non-Gaussian resource—small Schrödinger cat states—without post-selection, and it allows us to engineer larger amplitude cat states through two rounds of breeding[21]. Capitalizing on this and applying real-time feedforward, we achieve the quasi-deterministic generation of optical GKP states[22,23], a leading resource for bosonic quantum error correction.

Finally, Clavina can perform complex many-body quantum simulations, as exemplified by the Bose–Hubbard model[24], beyond the constraints of purely linear optics. By connecting the programmable linear network to a tunable Kerr interaction[15], we can encode all the boson-lattice parameters. When combined with photon-number-resolving detectors (PNRDs), this enables simulations of quantum dynamics beyond the hard-core boson limit (with more than one boson per site). This regime is inherently challenging for superconducting platforms, as their on-site interactions are not tunable. These capabilities establish a new experimental paradigm for many-body simulations and provide an all-optical pathway to photonic universal quantum simulation.

Extensible photonic quantum processor

We illustrate the composability and extensibility of Clavina in Fig. 1a as a jigsaw, assembled piece by piece. This extensibility allows us to add new functionality to the circuit without a complete overhaul of the design. A central CU—comprising phase-locking, a cache (a long-fibre delay line) and synchronization modules—dispatches control signals to all the active components and schedules their tasks and operation sequences. The combination of time-bin encoding[13,25,26] and a loop-based architecture[11] allows functional modules to be located along a single optical path. Each module can be reused to perform operations on successive time bins, as programmed by the CU. The capabilities of the system could be extended by adding more modules via the input and output ports of the CU. Quantum states of light can be selected from coherent, squeezed or heralded photon-number states, and detectors can be chosen from superconducting nanowire single-photon detectors (SNSPDs), PNRDs or homodyne detectors (HDs). In addition, a linear operation unit (LOU), which supports several computational cores, shortens the overall optical path length for the same circuit depth and, together with phase-stabilized delay lines, implements large-scale linear transformations.

Notably, this architecture enables us to fulfil the hardware requirements for a universal physical gate set with a nonlinear unit (NLU). It incorporates a Kerr gate[15], coupled via the CU to the LOU, and, thus, overcomes the limitations of solely linear operations. This satisfies the universality requirement in the continuous-variable setting, which demands access to both Gaussian and non-Gaussian resources[16–18]. With this flexible and extensible architecture, other functional modules can be integrated in a plug-and-play manner. This makes Clavina an upgradable photonic quantum computing system suitable for a variety of applications, including quantum computing, simulation and machine learning (Fig. 1b). For more details of the experimental set-up and applications, see Supplementary Sections II–IV.

The scalability and full programmability of Clavina were demonstrated using a dual-core LOU (Fig. 2a), which maintained high phase stability over long operating times (Fig. 2b). As a benchmark, we performed a 100-mode Gaussian boson sampling experiment. This sampling task relies on tunable squeezed-state inputs and a fully reconfigurable interferometer, thereby providing a stringent test of adjustable squeezing and programmable linear-optical control. We used this experiment to evaluate the participation coefficients of a network[11,27], the results of which are shown in Fig. 2c. In addition, Clavina readily time-multiplexes squeezed light pulses to generate scalable cluster

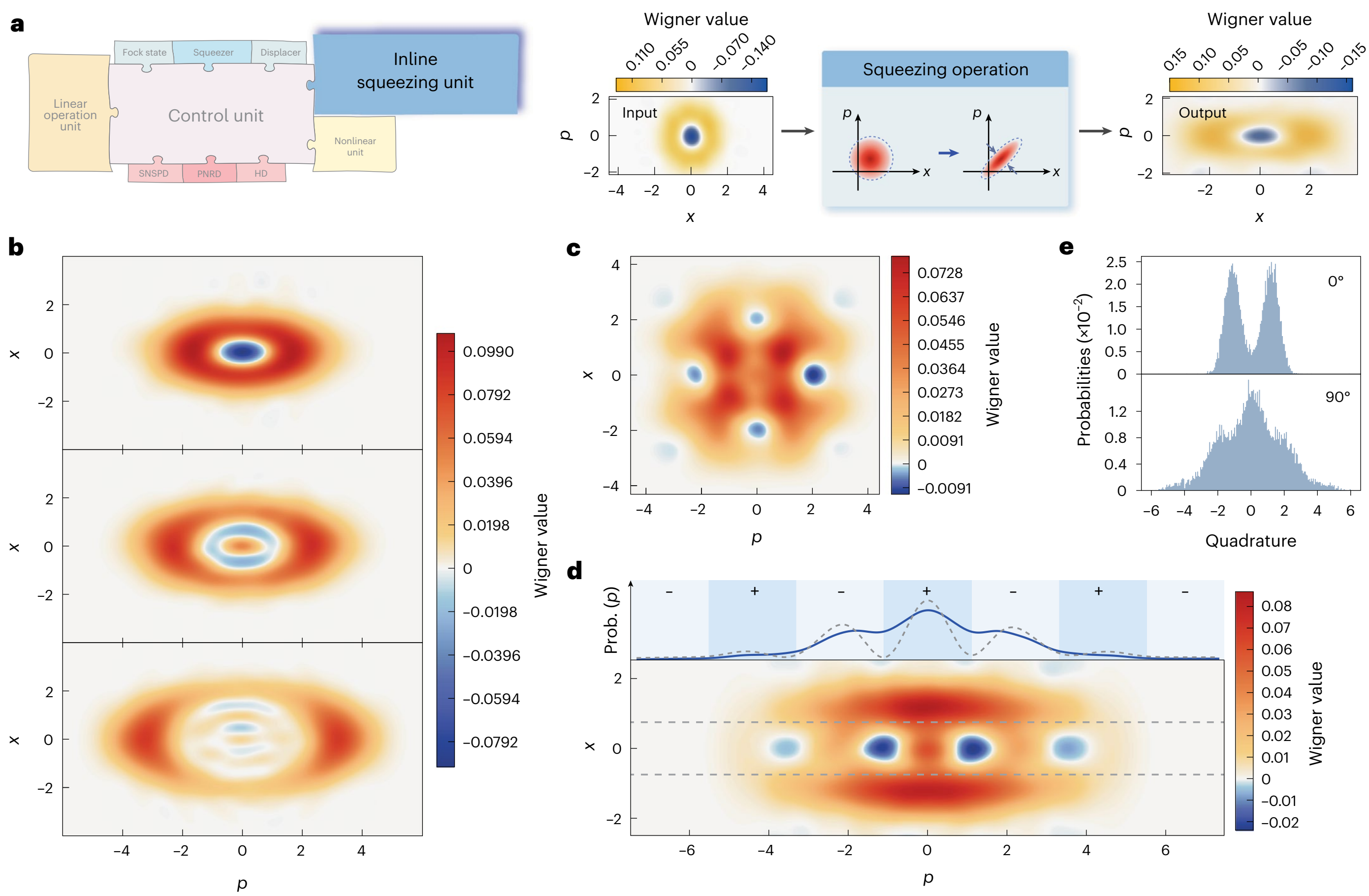

Fig. 3 | Engineering non-Gaussian resources for quasi-deterministic GKP state generation. a, An inline squeezer[20] acting on a single-photon state can produce a state that serves as a small cat state, which can then be used as a resource for generating GKP codes. **b**, Outcomes when breeding Schrödinger cat states. An initial small cat state (top) is prepared by the inline squeezing of a single-photon Fock state with a squeezing parameter $r \approx 0.3$. It is then expanded into a larger amplitude cat state through iterative breeding (middle: after one round; bottom: after two rounds). **c**, The Wigner function of the optical compass state is reconstructed from the interference of two cat states, prepared with an inline squeezing of $r = 0.6$. **d**, Quasi-deterministic generation of the GKP grid state. The marginal probabilities (prob.), shown as a solid blue line for the full dataset and a grey dashed line for the subset filtered to $|x| < 0.75$, reveal a phase-space lattice of peaks and troughs characteristic of a logical grid state. The initial cat state is prepared using an inline squeezing of $r = 0.48$. **e**, Measured quadrature probability distributions for the GKP state along two orthogonal phase quadratures (0 and π/2 cuts). More details are given in Supplementary Section VI.B.

states[28,29]. Figure 2d,e confirms the quantum correlations across 8,000 time bins. More information can be found in Supplementary Section VI.

Beyond linear operations, the extensibility of Clavina offers two routes to introducing the tunable nonlinear resources required for universality. First, nonlinear resource states, such as photon-number states, can be injected at the input and then subjected to inline squeezing via the inline squeezing unit (ISU). Second, the NLU can apply a Kerr gate to the circulating states. The loop-based architecture allows individual time bins to be arbitrarily switched into either unit, depending on the application. This flexibility in interleaving the ISU and the NLU with LOU executions enables a variety of computational tasks and substantially advances the realization of future universal fault-tolerant photonic quantum computers. In the following sections, we demonstrate the utility of these resources for GKP state engineering and for simulating a Bose–Hubbard model.

Non-Gaussian state engineering

Nonlinear resources are essential for generating non-Gaussian quantum states and universal quantum computing, but they are challenging to implement in photonic systems due to the absence of natural photon–photon interactions. Current demonstrations rely either on light–matter interactions[30] or measurement-induced schemes[31,32], but these approaches are typically weak[19] or probabilistic, respectively.

Here we employ a boosted[33] heralded photon-number-state generator to produce these nonlinear resource states near deterministically (Supplementary Fig. 3). Prepared at a rate of 1 MHz, they were switched into the ISU[20], which generated odd-parity Schrödinger cat states, as shown in Fig. 3a. The boosted heralding efficiency was approximately 93%. Taking the residual circuit loss into account, we estimated the effective output rate to be~0.85 MHz (Supplementary Section II.C). Enabled by the interferometric stability of Clavina, a subsequent two-round breeding process was performed in the LOU, in which the amplitude of interfering pairs of small cat states was increased to generate larger cat states[34]. The Wigner tomography[35] results in Fig. 3b confirm both the growth in amplitude and the preservation of Wigner negativity. With a modified heralding pattern—by conditioning on a two-photon detection event in the heralding PNRD arm—the same breeding protocol can prepare a compass state, which is a four-component coherent state superposition, as shown in Fig. 3c.

Quasi-deterministic generation of an optical GKP state

The cat states prepared above enable the synthesis of an optical GKP state[4,23]. With Clavina, several cat states can interfere with each other in the LOU while each ancilla bin is monitored by one HD. The measurement outcomes of the ancilla time bins are fed forward to a real-time

https://doi.org/10.1038/s41566-026-01962-8

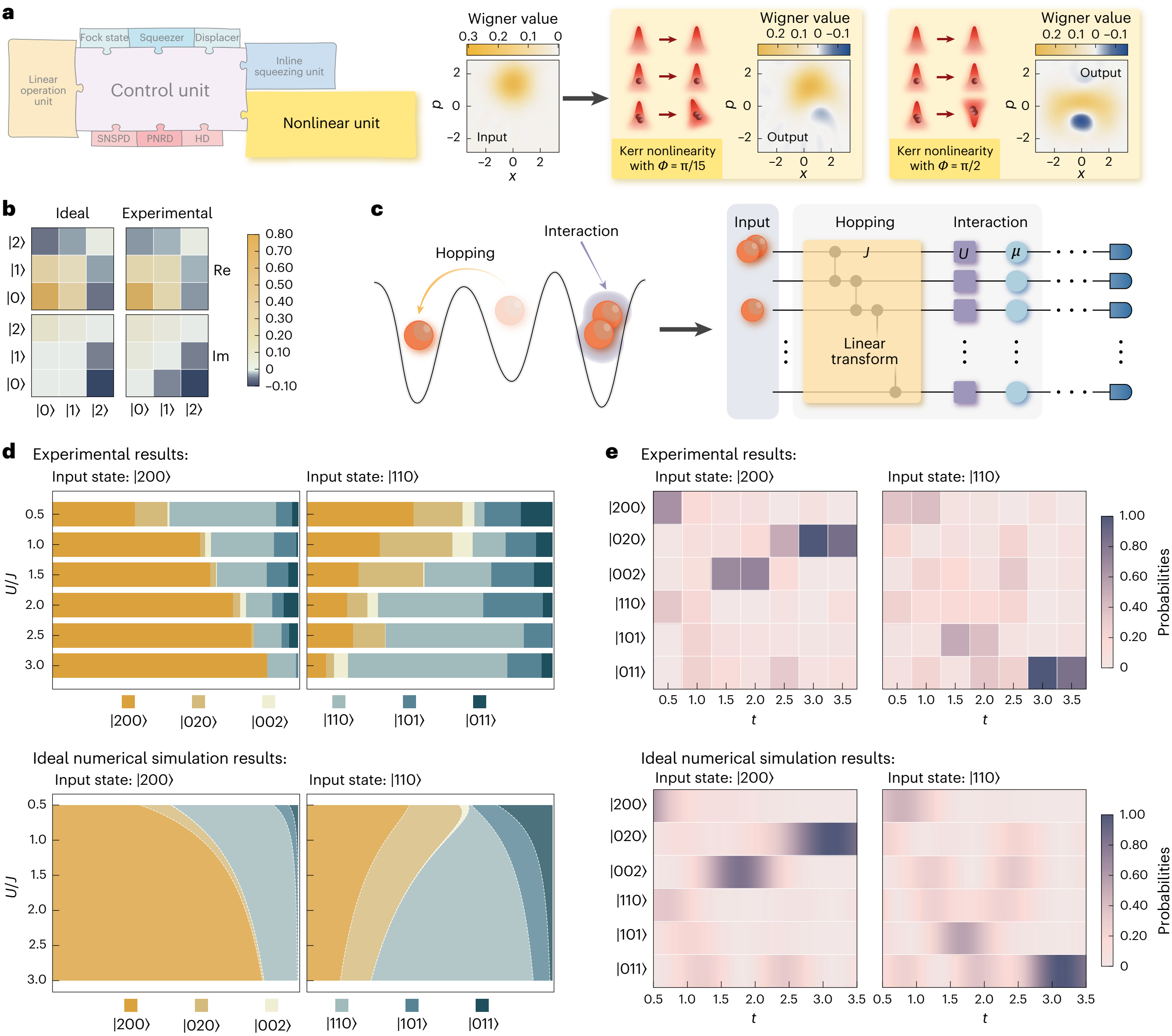

Fig. 4 | Nonlinear resource for simulating a Bose–Hubbard Hamiltonian. **a**, A measurement-induced Kerr interaction ($e^{-i\hat{H}t/\hbar}$)[15], with Hamiltonian $\hat{H} = \hbar\kappa\hat{n}(\hat{n}-1)$ (where $\hat{n}$ is the bosonic number operator, κ is Kerr nonlinear interaction strength and $\hbar$ is the reduced Planck constant), directly introduces nonlinearity by imparting a phase shift of $\Phi = \kappa t$ to the two-photon component relative to the zero- and one-photon components, as evidenced by the Wigner negativity (blue regions) of the output state. **b**, Fidelity of the Kerr interaction in the low-photon-number Fock subspace reached 0.820 ± 0.033 relative to the real (Re) and imaginary (Im) component of ideal values, for a coherent-state input with $\alpha = 0.5$ and Kerr nonlinearity $\Phi = \pi/3$. **c**, Schematic of the one-dimensional Bose–Hubbard model, where bosons (for example, photons) hop between nearest-neighbour lattice sites and experience on-site interactions. This model can be simulated with Clavina by interfacing the NLU with the LOU via the central CU. The LOU implements the hopping term J by coupling time-bin modes, analogous to tunnelling between neighbouring sites. The NLU enables the on-site interaction U. For simplicity, the on-site potential term μ is set to zero. **d**, Occupation probabilities after a fixed evolution time ($t = 0.5$) while the interaction-to-tunnelling ratio U/J is swept from 0.5 to 3.0. Each bar is stacked according to the six two-photon Fock configurations. Left and right subpanels correspond to the initial states |200⟩ and |110⟩, respectively. **e**, Time-resolved evolution at $U/J = 1$. The heat maps show the same Fock-state probabilities as functions of time for the two initial states used in **d**. Top: experimental results. Bottom: ideal numerical simulations sampled densely across U/J and t. The observed agreement, within experimental uncertainty, demonstrates that Clavina accurately captures the dynamics.

displacement operation on the remaining time bin. This allows a GKP state to be produced quasi-deterministically[36], a key breakthrough towards practical quantum error correction. Although recent probabilistic GKP state preparation schemes[2,4,37] have brought about notable advances, our architecture offers a deterministic approach, in principle, thus enabling the generation of cat states without post-selection and incorporating feedforward conditioned on homodyne outcomes[36]. In practice, we filter out homodyne outcomes with excessive noise arising mainly from the limited throughput and squeezing available in the current implementation. As such, the system is constrained to the quasi-deterministic generation of GKP states. By operating the experiment at 250 kHz, we generated approximately 2,000 GKP states per second.

Figure 3d shows the one-dimensional GKP state we measured with the quadrature distributions shown in Fig. 3e (Supplementary

Section VI.B). This reconstructed Wigner function exhibits the characteristic grid pattern, consistent with an approximate GKP logical state. We assessed the quality of this GKP state by measuring the stabilizer amplitudes $\langle \hat{S}_x \rangle = 0.1061 \pm 0.0071$ and $\langle \hat{S}_{|1_L\rangle} \rangle = 0.2065 \pm 0.0055$. These results show that the state had preserved appreciable lattice-wide phase coherence while suppressing the logical-Z component, as expected for the $|1_L\rangle$ codeword. Independent confirmation comes from the quadrature variances of the central lattice peak, $\langle \Delta^2 x \rangle = 0.1493 \pm 0.0052$ and $\langle \Delta^2 p \rangle = 0.0870 \pm 0.0018$. The product, $\langle \Delta^2 x \rangle \langle \Delta^2 p \rangle = 0.0130 \pm 0.0005$, is more than an order of magnitude below the vacuum limit, which confirms the presence of sub-Planck-scale interference fringes characteristic of an ideal grid state[38]. Further details, such as stabilizer definitions and effective peak squeezing, are provided in Supplementary Section VI.

As with previous demonstrations[2,4], lower loss and higher squeezing are required for these states to be practically useful for error correction. Despite this, the relatively large stabilizer amplitudes, together with a sharply localized peak, indicate that the state cannot be reproduced with Gaussian resources alone. Moreover, its quasi-deterministic generation from a near-on-demand non-Gaussian resource (Fock states) makes this approach a promising route to fault-tolerant quantum computing via further Gaussian operations[39].

Photonic quantum many-body simulations

We now describe our NLU, which comprises a strong Kerr interaction realized by interferometrically combining photon-addition and photon-subtraction sequences[14,15] (Supplementary Section IV.B). Owing to the extensible design of Clavina, the NLU was easily interfaced with the LOU to induce a strong nonlinearity, as shown in Fig. 4a. The fidelity of the Kerr interaction is quantified in Fig. 4b. The NLU provides the essential non-Gaussian element that, together with our Gaussian toolbox, completes the hardware-level gate set for universal quantum computing. This capability allows Clavina to directly simulate the dynamics of an interacting many-body system, moving beyond the constraints of linear-optical networks. As a demonstration, we simulated a three-site Bose–Hubbard model using a three-mode version of the circuit[40] (Fig. 4c).

Our architecture enables the real-time observation of Bose–Hubbard dynamics while allowing us to tune the interaction-to-tunnelling ratio U/J and the evolution time t. The LOU implements the hopping term J by coupling time-bin modes, analogous to tunnelling between neighbouring sites, while the NLU enables the on-site interaction, U. The on-site potential term μ, which can be controlled by a local phase shift, is set to zero for simplicity. For these demonstrations, we initialized two photons in the chosen Fock states and then measured their distributions. Figure 4d demonstrates that the preferred photon-occupancy pattern depends jointly on the interaction ratio U/J and the initial state. Starting from the bunched state $|200\rangle$ at a fixed evolution time $t = 0.5$, weak interactions populated both bunched and separated configurations, whereas increasing U/J stabilized double-occupancy and suppressed singly occupied states. The trend was reversed for the initial state $|110\rangle$, as weak interactions favoured doubly occupied states, while increasing U/J kept the photons apart. Consistent with expectations, a large J enhanced hopping, resulting in contrasting behaviours for the two initial states. Figure 4e shows the dynamics with $U = J$. For different initial states, we tracked the state populations over $t \in [0.5, 3.5]$. After a long period of evolution, the dynamics show an initialization-dependent preference for either bunched or separated configurations. Further details are provided in Supplementary Section VII.

Compared with superconducting and other physical platforms, Clavina offers several distinct advantages. Benefiting from fast electro-optic modulation, the circuit can be reconfigured on the fly, making both the couplings J_{ij} and the on-site interactions U tunable in time. Such capabilities are typically challenging to realize in superconducting-qubit architectures[41], where U is generally fixed at a large value and cannot be tuned, thereby restricting simulations to the hard-core boson limit (within a perturbative regime). On our platform, we can explore finite-U physics and, by leveraging PNRDs, directly probe multi-occupancy beyond that regime. Collectively, these capabilities establish our photonic realization of this type of many-body model as a practical pathway to scalable photonic quantum simulators[42–44].

Discussion and outlook

To overcome the long-standing limitation of photonic quantum computing to linear operations, we propose an extensible architecture that integrates scalable linear networks with diverse nonlinear functional modules. We apply an inline squeezer to Fock states and a nonlinear Kerr gate, both of which are crucial for advancing towards universality. The measurement-induced approach used in our work circumvents the intrinsic limitations identified in ref. 19 by avoiding direct Kerr nonlinearities and, thus, the causality-induced phase noise that compromises high-fidelity operation. This approach can also be extended naturally to the multiphoton case[45], thereby enabling strong nonlinearities at higher photon numbers. For near-term implementations, alongside continuing improvements in gate fidelity, the probabilistic nature can be mitigated by offline preparation buffered in a fibre-delay loop using a repeat-until-success strategy; the prepared gate is then injected into the main circuit via gate teleportation to enable near-deterministic and scalable operation. Furthermore, photon addition and subtraction can be achieved deterministically via light–matter interfaces[46], for instance, using semiconductor quantum dots[47]. The engineered quantum-dot devices can act as single-photon adders[48,49] or subtractors[50] on each time-bin mode, thereby providing a nonlinear resource while preserving the modularity of the platform.

In the long term, direct Kerr-like interactions may also become feasible. Although ref. 19 argued that single-photon Kerr nonlinearity cannot be achieved with high fidelity under realistic conditions, recent progress indicates that there is no fundamental barrier to such operations. Platforms like strongly coupled photonic crystal microcavities[51], hybrid Rydberg-atom systems[52] and waveguide-embedded quantum dots[53] are steadily advancing towards significant single-photon-level nonlinearities, indicating that high-fidelity Kerr or other nonlinear gates could eventually be realized. Importantly, these platforms are naturally compatible with the extensible time-bin loop architecture of Clavina, which allows each time bin to interact sequentially with a shared NLU for scalable, hardware-efficient nonlinear processing.

In this work, we have demonstrated the generation of GKP states, which lays the groundwork for producing states characterized by large amplitudes and high squeezing levels[54]. The approach to time-bin encoding in Clavina[28,29] is naturally suited for generating large-scale GKP cluster states and constructing surface codes[12], a crucial requirement for concatenating with topological error-correcting codes to achieve fault tolerance. Consequently, our architecture offers a promising route towards active quantum error correction (Supplementary Section VI.C).

To move towards fault-tolerant universality, the physical non-Gaussian resources demonstrated here must be integrated with tailored error-correcting codes to fully exploit gate transversality. Specifically, high-fidelity GKP states serve as the foundational logical Pauli states. Our NLU can supply the essential non-Clifford physical operations required to generate and distil magic states, thereby completing the universal logical gate set that transversal operations alone cannot provide.

Finally, Clavina is readily transferable to integrated photonic circuits—for example, those based on thin-film lithium niobate on insulator—which are capable of fast electro-optic modulation and integrated high-gain squeezing. Integrating these sources with time-bin circuitry on-chip would help to mitigate some of the photon losses associated with coupling to optical fibre[55,56].

With continued advances in component engineering and quantum error correction, the blueprint realized in Clavina can be refined into a fault-tolerant universal photonic quantum computer, thereby positioning photonic systems as compelling candidates for next-generation quantum technology.

Online content

Any methods, additional references, Nature Portfolio reporting summaries, source data, extended data, supplementary information, acknowledgements, peer review information; details of author contributions and competing interests; and statements of data and code availability are available at https://doi.org/10.1038/s41566-026-01962-8.

References

1. Rad, H. A. et al. Scaling and networking a modular photonic quantum computer. *Nature* **638**, 912–919 (2025).
2. Larsen, M. V. et al. Integrated photonic source of Gottesman–Kitaev–Preskill qubits. *Nature* **642**, 587–591 (2025).
3. PsiQuantum Team A manufacturable platform for photonic quantum computing. *Nature* **641**, 876–883 (2025).
4. Konno, S. et al. Logical states for fault-tolerant quantum computation with propagating light. *Science* **383**, 289–292 (2024).
5. Bente, I. et al. The potential of multidimensional photonic computing. *Nat. Rev. Phys.* **7**, 439–450 (2025).
6. O'Brien, J. L., Furusawa, A. & Vučković, J. Photonic quantum technologies. *Nat. Photonics* **3**, 687–695 (2009).
7. Bartolucci, S. et al. Fusion-based quantum computation. *Nat. Commun.* **14**, 912 (2023).
8. Maring, N. et al. A versatile single-photon-based quantum computing platform. *Nat. Photonics* **18**, 603–609 (2024).
9. Kawasaki, A. et al. Real-time observation of picosecond-timescale optical quantum entanglement towards ultrafast quantum information processing. *Nat. Photonics* **19**, 271–276 (2025).
10. Lib, O. et al. Resource-efficient photonic quantum computation with high-dimensional cluster states. *Nat. Photonics* **18**, 1218–1224 (2024).
11. Yu, S. et al. A universal programmable Gaussian boson sampler for drug discovery. *Nat. Comput. Sci.* **3**, 839–848 (2023).
12. Noh, K. & Chamberland, C. Fault-tolerant bosonic quantum error correction with the surface-Gottesman–Kitaev–Preskill code. *Phys. Rev. A* **101**, 012316 (2020).
13. Madsen, L. S. et al. Quantum computational advantage with a programmable photonic processor. *Nature* **606**, 75–81 (2022).
14. Biagi, N., Francesconi, S., Zavatta, A. & Bellini, M. Photon-by-photon quantum light state engineering. *Prog. Quantum Electron.* **84**, 100414 (2022).
15. Costanzo, L. S. et al. Measurement-induced strong Kerr nonlinearity for weak quantum states of light. *Phys. Rev. Lett.* **119**, 013601 (2017).
16. Lloyd, S. & Braunstein, S. L. Quantum computation over continuous variables. *Phys. Rev. Lett.* **82**, 1784 (1999).
17. Bartlett, S. D. & Sanders, B. C. Universal continuous-variable quantum computation: requirement of optical nonlinearity for photon counting. *Phys. Rev. A* **65**, 042304 (2002).
18. Braunstein, S. L. & van Loock, P. Quantum information with continuous variables. *Rev. Mod. Phys.* **77**, 513 (2005).
19. Shapiro, J. H. Single-photon Kerr nonlinearities do not help quantum computation. *Phys. Rev. A* **73**, 062305 (2006).
20. Miwa, Y. et al. Exploring a new regime for processing optical qubits: squeezing and unsqueezing single photons. *Phys. Rev. Lett.* **113**, 013601 (2014).
21. Jeong, H., Lund, A. P. & Ralph, T. C. Production of superpositions of coherent states in traveling optical fields with inefficient photon detection. *Phys. Rev. A* **72**, 013801 (2005).
22. Gottesman, D., Kitaev, A. & Preskill, J. Encoding a qubit in an oscillator. *Phys. Rev. A* **64**, 012310 (2001).
23. Vasconcelos, H. M., Sanz, L. & Glancy, S. All-optical generation of states for 'Encoding a qubit in an oscillator'. *Opt. Lett.* **35**, 3261–3263 (2010).
24. Bloch, I., Dalibard, J. & Zwerger, W. Many-body physics with ultracold gases. *Rev. Mod. Phys.* **80**, 885 (2008).
25. Yonezu, K., Enomoto, Y., Yoshida, T. & Takeda, S. Time-domain universal linear-optical operations for universal quantum information processing. *Phys. Rev. Lett.* **131**, 040601 (2023).
26. Enomoto, Y., Yonezu, K., Mitsuhashi, Y., Takase, K. & Takeda, S. Programmable and sequential Gaussian gates in a loop-based single-mode photonic quantum processor. *Sci. Adv.* **7**, eabj6624 (2021).
27. Yu, S. et al. Topological network analysis using a programmable photonic quantum processor. Preprint at https://arxiv.org/abs/2507.08157 (2025).
28. Asavanant, W. et al. Generation of time-domain-multiplexed two-dimensional cluster state. *Science* **366**, 373–376 (2019).
29. Larsen, M. V., Guo, X., Breum, C. R., Neergaard-Nielsen, J. S. & Andersen, U. L. Deterministic generation of a two-dimensional cluster state. *Science* **366**, 369–372 (2019).
30. Chang, D. E., Vuletić, V. & Lukin, M. D. Quantum nonlinear optics—photon by photon. *Nat. Photonics* **8**, 685–694 (2014).
31. Patel, R. B., Ho, J., Ferreyrol, F., Ralph, T. C. & Pryde, G. J. A quantum Fredkin gate. *Sci. Adv.* **2**, e1501531 (2016).
32. O'Brien, J. L., Pryde, G. J., White, A. G., Ralph, T. C. & Branning, D. Demonstration of an all-optical quantum controlled-NOT gate. *Nature* **426**, 264–267 (2003).
33. Simon, H., Caron, L., Journet, R., Cotte, V. & Tualle-Brouri, R. Experimental demonstration of a versatile and scalable scheme for iterative generation of non-Gaussian states of light. *Phys. Rev. Lett.* **133**, 173603 (2024).
34. Sychev, D. V. et al. Enlargement of optical Schrödinger's cat states. *Nat. Photonics* **11**, 379–382 (2017).
35. Lvovsky, A. I. & Raymer, M. G. Continuous-variable optical quantum-state tomography. *Rev. Mod. Phys.* **81**, 299–332 (2009).
36. Weigand, D. J. & Terhal, B. M. Generating grid states from Schrödinger-cat states without postselection. *Phys. Rev. A* **97**, 022341 (2018).
37. Crescimanna, V., Yu, S., Heshami, K. & Patel, R. B. Adaptive non-Gaussian quantum state engineering. *Phys. Rev. A* **112**, 053705 (2025).
38. Zurek, W. H. Sub-Planck structure in phase space and its relevance for quantum decoherence. *Nature* **412**, 712–717 (2001).
39. Baragiola, B. Q., Pantaleoni, G., Alexander, R. N., Karanjai, A. & Menicucci, N. C. All-Gaussian universality and fault tolerance with the Gottesman–Kitaev–Preskill code. *Phys. Rev. Lett.* **123**, 200502 (2019).
40. Kalajdzievski, T., Weedbrook, C. & Rebentrost, P. Continuous-variable gate decomposition for the Bose–Hubbard model. *Phys. Rev. A* **97**, 062311 (2018).
41. Arute, F. et al. Quantum supremacy using a programmable superconducting processor. *Nature* **574**, 505–510 (2019).
42. Daley, A. J. et al. Practical quantum advantage in quantum simulation. *Nature* **607**, 667–676 (2022).
43. Aspuru-Guzik, A. & Walther, P. Photonic quantum simulators. *Nat. Phys.* **8**, 285–291 (2012).
44. Lloyd, S. Universal quantum simulators. *Science* **273**, 1073–1078 (1996).
45. Fadrný, J. et al. Experimental preparation of multiphoton-added coherent states of light. *npj Quantum Inf.* **10**, 89 (2024).
46. Luo, H., Shah, P. S., Yang, F., Mirhosseini, M. & Mahmoodian, S. Dynamic stimulated emission for deterministic addition and subtraction of propagating photons. Preprint at https://arxiv.org/abs/2512.09711 (2025).

https://doi.org/10.1038/s41566-026-01962-8

47. Uppu, R., Midolo, L., Zhou, Y., Carolan, J. & Lodahl, P. Femtosecond few-fermion dynamics and deterministic single-photon gain in a quantum dot. *Nat. Nanotechnol.* **16**, 1308–1317 (2021).
48. Sotier, F. et al. Femtosecond few-fermion dynamics and deterministic single-photon gain in a quantum dot. *Nat. Phys.* **5**, 352–356 (2009).
49. Steindl, P. et al. Artificial coherent states of light by multiphoton interference in a single-photon stream. *Phys. Rev. Lett.* **126**, 143601 (2021).
50. Lund, M. M., Yang, F., Christiansen, V. R., Kornovan, D. & Mølmer, K. Subtraction and addition of propagating photons by two-level emitters. *Phys. Rev. Lett.* **133**, 103601 (2024).
51. Hastrup, J. & Andersen, U. L. Protocol for generating optical Gottesman–Kitaev–Preskill states with cavity QED. *Phys. Rev. Lett.* **128**, 170503 (2022).
52. Tiarks, D., Schmidt-Eberle, S., Stolz, T., Rempe, G. & Dürr, S. A photon–photon quantum gate based on Rydberg interactions. *Nat. Phys.* **15**, 124–126 (2019).
53. Staunstrup, M. J. R. et al. Direct observation of a few-photon phase shift induced by a single quantum emitter in a waveguide. *Nat. Commun.* **15**, 7583 (2024).
54. Winnel, M. S., Guanzon, J. J., Singh, D. & Ralph, T. C. Deterministic preparation of optical squeezed cat and Gottesman–Kitaev–Preskill states. *Phys. Rev. Lett.* **133**, 230602 (2024).
55. Harris, T. B., Matsuura, T., Baragiola, B. Q. & Menicucci, N. C. Logical channel for heralded and pure loss with the Gottesman–Kitaev–Preskill code. *Phys. Rev. A* **112**, 042417 (2025).
56. Finco, G. et al. Time-bin entangled Bell state generation and tomography on thin-film lithium niobate. *npj Quantum Inf.* **10**, 135 (2024).
57. Yu, S. et al. Shedding light on the future: exploring quantum neural networks through optics. *Adv. Quantum Technol.* **8**, 2400074 (2025).
58. Yang, B. et al. Observation of gauge invariance in a 71-site Bose–Hubbard quantum simulator. *Nature* **587**, 392–396 (2020).

Publisher's note Springer Nature remains neutral with regard to jurisdictional claims in published maps and institutional affiliations.

Open Access This article is licensed under a Creative Commons Attribution 4.0 International License, which permits use, sharing, adaptation, distribution and reproduction in any medium or format, as long as you give appropriate credit to the original author(s) and the source, provide a link to the Creative Commons licence, and indicate if changes were made. The images or other third party material in this article are included in the article's Creative Commons licence, unless indicated otherwise in a credit line to the material. If material is not included in the article's Creative Commons licence and your intended use is not permitted by statutory regulation or exceeds the permitted use, you will need to obtain permission directly from the copyright holder. To view a copy of this licence, visit http://creativecommons.org/licenses/by/4.0/.

© The Author(s) 2026

Methods

Hardware summary

Clavina is an extensible photonic quantum computing platform composed of six units. Specifically, squeezed states are produced by a low-loss optical parametric oscillator, and photon-number states are prepared near-deterministically via heralding with a boosting protocol; both the squeezing level and the coherent-state amplitude are tuned by computer-controlled EOMs. The current implementation uses a dual-core, time-bin-encoded LOU, where each core consists of a pair of EOMs that implement SU(2) operations between adjacent time-bin modes. Other cores can be incorporated to realize larger linear transformations while reducing the number of loops required for a given circuit depth. The CU includes a phase-locked delay line, a long-fibre delay and an input/output module controlled by optical switches to provide time-bin synchronization and dynamic routing. This allows functional modules, such as the ISU and NLU, to be inserted or bypassed on a per-time-bin basis. This plug-and-play architecture enables efficient hardware reuse along a single optical path and supports flexible reconfiguration for various tasks. The output states are measured using SNSPDs, PNRDs or HDs. Over extended operation, the observed fidelity reduction (Fig. 2b) was probably caused by the cumulative effect of several minor drifts and imperfections. These include slight reductions in coupling efficiency, modest degradation of the interference extinction ratio in the LOU (despite active phase-locking), small drifts in EOM driver accuracy during long runs (possibly due to thermal effects) and slight variations in SNSPD detection efficiency over time. Although each of these effects is minor in isolation, their combined impact can become noticeable during longer measurements.

To reduce losses in the near term, we could use higher-bandwidth EOMs to increase the source repetition rate and shorten the temporal spacing between time bins. This would enable the use of shorter Herriott cells and allow free-space delays to replace the fibre delays, thereby eliminating the fibre-coupling loss entirely. Simultaneously, continuing improvements in photodetectors—including devices with efficiencies up to 99% and SNSPDs/PNRDs exceeding 95%—will directly reduce the read-out loss.

In the longer term, the Clavina architecture is inherently compatible with integrated photonics. Thin-film lithium niobate platforms, for instance, support 100–200 GHz modulation, which corresponds to picosecond-scale delays and millimetre-scale path lengths. Coupled with propagation losses as low as 0.01 dB cm^{-1}, monolithically integrating the ISU and NLU onto a single chip presents a promising route for substantially suppressing the coupling losses in the current bulk-optic implementation.

GKP state preparation

The preparation of GKP states requires that nonlinear resources are added to a linear-optical system. Two main approaches can achieve this: photon-number-state injection and photon-number-state detection (the strategy used in ref. 2). Both combine photon-number-induced nonlinearity with linear operations, like inline squeezing and beam-splitter interference, but differ in where the nonlinearity is introduced. Detection relies on post-selected, photon-number-resolved outcomes. Although intrinsically probabilistic, this is a practical way to scale nonlinear resources by selecting higher photon-number sampling events. For example, ref. 2 produced a two-dimensional GKP state with three lobes along both the x- and p-quadratures by post-selecting on 3-3-3 photon-sampling outcomes (equivalent to a nine-photon nonlinear resource). By contrast, injection introduces non-Gaussian resources directly via prepared single-photon inputs. Combined with inline squeezing and interference, injection enables deterministic operation in principle, assuming idealized limits without finite squeezing constraints or loss.

Generally, the amount of nonlinear resource dictates the size of the generated GKP state, whereas the achievable squeezing and losses limit its quality. In this work, four squeezed single-photon inputs provided the equivalent of a four-photon nonlinear resource, yielding a one-dimensional GKP state. Although capable of correcting small displacement errors along the p-quadrature, this does not realize a full two-dimensional, fault-tolerant GKP state. Nevertheless, the injection architecture is fundamentally scalable: increasing the single-photon inputs and breeding steps can generate larger two-dimensional GKP states, although mitigating the fidelity-reducing effects of further losses remains a practical challenge.

Data availability

Source data are provided with this paper. All other data related to this study are available from the corresponding authors upon reasonable request.

Acknowledgements

We thank B. Q. Baragiola, Z. Yin, Z. Jia, Z. Li, M. Bellini, Z.-H. Liu, Z.-P. Zhong, A. Zhang and Z. Zhu for helpful discussions and feedback on the paper. We also acknowledge Zhejiang Lab for providing access to shared research facilities that supported this work.

Author contributions

S.Y. and R.B.P. designed the project. S.Y., R.B.P. and Z.-H.Y. built and operated the experiments with the help of K.-C.C., G.Y., Z.L., E.M., G.J.M. and I.A.W. S.Y. and R.B.P. designed the cat state breeding and GKP generation circuits and completed the corresponding data analysis with the help of K.-C.C., Z.L., M.S.K., J.S., E.M., Y.K.A., G.J.M., K.-C.C., S.H.W., D.M.L. and Z.C.-Z. J.S., S.Y., Y.D. and R.B. conceived the theoretical model and circuits of the Bose–Hubbard Hamiltonian simulation. J.S., S.Y., R.B., Y.D., V.V., M.Z., K.-C.C., S.H.W. and D.M.L. completed the corresponding data analysis. S.Y., J.S., R.B.P., K.-C.C. and Z.L. prepared the article with input from all authors.

Funding

This work was supported by a UK Research and Innovation Guarantee Postdoctoral Fellowship (Project No. EP/Y029631/1) and Future Leaders Fellowship (Project No. MR/W011794/1), The Royal Society (Project No. RG\R2\232514), the Engineering and Physical Sciences Research Council hub for Quantum Computing via Integrated and Interconnected Implementations (Project No. EP/Z53318X/1), Distributed Quantum Computing and Applications (Project No. EP/W032643/1), NSFC (No. 12475042), National Key R&D Program of China (No. 2023YFF0718400), Schmidt Sciences, EU Horizon 2020 Marie Sklodowska-Curie Innovation Training Network (Project No. 956071, AppQInfo) and the National Research Council of Canada (Project No. QSP 062-2).

Competing interests

The authors declare no competing interests.

Additional information

Supplementary information The online version contains supplementary material available at https://doi.org/10.1038/s41566-026-01962-8.

Correspondence and requests for materials should be addressed to Shang Yu, Jinzhao Sun, Ying Dong or Raj B. Patel.

Peer review information *Nature Photonics* thanks Massimo Borghi and David Herrera-Martí for their contribution to the peer review of this work. Peer reviewer reports are available.

Reprints and permissions information is available at www.nature.com/reprints.